Received June 10, 2019, accepted June 23, 2019, date of publication July 1, 2019, date of current version July 17, 2019.

Digital Object Identifier 10.1109/ACCESS.2019.2925894

A Hybrid Path Planning Method for an Unmanned Cruise Ship in Water Quality Sampling

JIABIN YU, WEI DENG, ZHIYAO ZHAO, XIAOYI WANG, JIPING XU, LI WANG, QIAN SUN, AND ZHE SHEN

School of Computer and Information Engineering, Beijing Technology and Business University, Beijing 100048, China

Corresponding authors: Zhiyao Zhao (zhaozy@btbu.edu.cn) and Xiaoyi Wang (wangxy@btbu.edu.cn)

This work was supported in part by the Beijing Natural Science Foundation under Grant 4194074, in part by the National Natural Science Foundation of China under Grant 61802010 and Grant 61703008, and in part by the Beijing Municipal Education Commission Research Program-General Project under Grant KM201910011011.

ABSTRACT Cruise ships are widely used in water quality monitoring but suffer from path planning problems in a surface water environment. Solutions to path planning problems have higher requirements of path planning distance and path planning time and the ability of real-time obstacles avoidance. This paper introduces a hybrid path planning method to solve the path planning problem when using unmanned cruise ships. First, a model of the surface water environment with unknown districts is established by the grid method. Then, the global path is planned by the A* algorithm based on such a model, and in unknown areas of the model, the artificial potential filed (APF) is employed for local path planning. The problem of obtaining unreachable targets and falling into a local minimum introduced by the APF is improved by using the optimized repulsion potential field function and adding the directional random escape strategy. The A* algorithm with self-learning ability is proposed for secondary planning and cases where a local path cannot be generated. Finally, the optimal path combined with the global path and the local path is smoothed. The simulation results show that the proposed algorithm has better performance than other algorithms from the aspects of distance cost and time cost.

INDEX TERMS Artificial potential field method, A* algorithm, hybrid path planning, obstacle avoidance, water quality sampling cruise ship.

I. INTRODUCTION

Unmanned cruise ships, surface mobile devices that can be autonomously cruised, are widely used for water quality sampling in public waters. The traditional mode employed by water sampling cruise ships is to reach the designated water sampling area via remote control. This method is simple, but for a larger water area, effective control is difficult because of limits of observation distance and communication distance. Autonomous cruise mode overcomes this limitation because a cruise ship has a navigation system, detection system, sampling system, and power system, so that the ship can auto cruise to the specified location to complete the water sampling task. Improvements in the planning method for autonomous cruise ships will allow a cruise ship to independently plan the optimal driving path in a short period of time and quickly identify and evade sudden-appearing unknown obstacles.

Path planning has been an active research topic since 1970s [1]. Path planning research can be divided into global path planning and local path planning from the perspective of target range [2]. Global path planning can achieve better characteristics in path distance based on global information. Several algorithms are proposed for this area, such as Dijkstra algorithm [3], A* algorithm [4], particle swarm optimization (PSO) [5], genetic algorithm (GA) [6], ant colony optimization (ACO) [7], [8], and grey wolf optimization (GWO) algorithm [9], *etc*. On the other hand, local path planning has outstanding performance in terms of path planning time. The commonly used methods include the artificial potential field (APF) method [10], [11], fuzzy logic based methods [12], and artificial neural network (ANN) [13]. In addition, there are many studies which usually use fusion approaches to compensate for the shortcomings brought by a

The associate editor coordinating the review of this manuscript and approving it for publication was Yingxiang Liu.

single algorithm. For global path planning, a mixture of A* algorithm and ACO shows good obstacle avoidance characteristics in complex environment [14]; an integration of PSO and Dijkstra algorithm obtains less path distance cost [15]; and ACO combined with PSO possess an ability to explore the environment including a small range of unknown regions [16]. However, such combinations increase the burden of path planning time and the real-time performance cannot be guaranteed. For local path planning, a combination of ANN and reinforcement learning algorithm has advantages in accomplishing optimal path in unknown environments [17]; a mixture of the dynamic windows approach and fuzzy logic has good response to avoid dynamic obstacles [18]; a hybrid algorithm of ANN and fuzzy logic obtains less path planning time [19]. However, the path planning distance could be further optimized and such combined methods lack good application in complex environment.

A hybrid algorithm containing global path planning and local path planning methods could aggregate advantages of each method [20]. Combined with the characteristics of the two type algorithms, a hybrid method has an ability to deal with path planning problem under complex unknown environments, reduce the path planning distance, and decrease the path planning time, which a simple combination of single-type algorithms cannot be achieved [21].

As for global path, sample-based path planning methods in global path planning, such as rapidly-exploring random tree (RRT) and probabilistic roadmap (PRM) can obtain the planning results in a relatively short time. However, the optimal path obtained only get sub-optimal solution in the path planning distance [22]. When the planning path needs to pass through the environment with dense obstacles or narrow channels, the planning efficiency of the algorithm will be reduced. Thus, the application of such algorithms has limitations in the circumstance of complex environment and unknown environment [23]. The A* algorithm which overcomes such disadvantages, is a classical global path planning algorithm with short computation time, high efficiency, and a simple structure for dealing with known environmental circumstance. However, in the face of unknown environmental circumstance, the repeated use of the A* algorithm is inefficient due to extended path planning time. The APF method is suitable for local path planning and real-time obstacle avoidance requirement due to its characteristics of short planning time and smooth planned path. However, the APF method has disadvantages of falling into a local minimum, and even a potentially unreachable target. Since the A* algorithm and the APF method have complementary characteristics, Wang [24] decomposed the path obtained by the A* algorithm into multiple sub nodes, and the APF method treated the sub nodes as the sub goals to obtain the optimal path. Kao et al. [25] used the A* algorithm to set local target points in unknown environments, and then used the APF method to solve the problem of obtaining unreachable targets. Park and Kim [26] used the A* algorithm with B-Spline curve to solve the locally optimal result brought by the APF method. However, these methods may show limitations in a complex environment with unknown areas.

Therefore, a hybrid path planning algorithm is proposed in this paper, which can deal with the circumstance of complex environment with unknown obstacles and find an optimal path in a short time. The A* algorithm is adopted for global path planning, and the APF method is used to achieve obstacle avoidance in an unknown environment. Then, by using the improved repulsive potential filed function and adding the directional random escape strategy, the problems of obtaining unreachable targets and falling into a local minimum for the APF are effectively solved. Further, the optimal path is smoothed to decrease the path planning distance and reduce steering angle of cruise ships. Finally, several comparative simulations are presented to show the effectiveness and advantageous performance of the proposed method.

The main contributions of this work can be summarized as follows: (1) the hybrid algorithm proposed in this paper combines the advantages of the A* algorithm and the APF method that can obtain feasible paths when facing with unknown or partially known environments; (2) the APF method, part of the proposed hybrid algorithm, is modified to deal with problems of obtaining unreachable targets and falling into a local minimum; (3) the hybrid algorithm proposed in this paper has a sensor-based self-learning ability which can better solve path planning problems in complex environments.

II. PREREQUISITE KNOWLEDGE

A. PUBLIC WATER MAP CONSTRUCTION

This research uses real water areas as the experimental environments. The obstacles in the waters include reefs, buoys, and groups of water grass. The six-rotor UAV is equipped with a camera for aerial photography, and the aerial photos are converted into simulation environment information through image processing technology [27]. The grid method is used to transform the environment information into a map model consisting of two-dimensional spatial grids that are connected and not overlapping [28], as shown in Figure 1. The grid map and the passable area are represented by a black and white rectangular grid, respectively, in Figure 1. The obstacle is used as the center of the circle, and the safety distance is 3 m to represent the obstacle area. When the obstacle area is less than one grid size, it is complemented by a grid. Some areas in the photos are difficult to identify by image processing because of camera resolution that limits image sharpness. These regions are marked as unknown environments and represented by a gray rectangular grid in the map but assumed to be passable areas, like the white grid, before it is explored. If there is an obstacle in the grid after the detection, it will be replaced by black rectangular grids; otherwise, it will still be gray.

B. THE A* ALGORITHM

The A* algorithm is a classical heuristic search algorithm based on the Dijkstra algorithm combined with the best

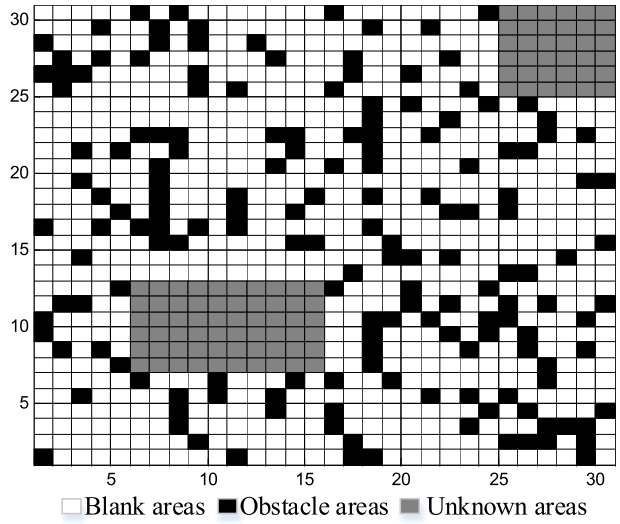

FIGURE 1. 30 × 30 grid map.

priority algorithm (BPA). The A* algorithm is mainly used to solve the optimal path problem from the starting point to the target in global path planning [29]. The method continuously approximates the target by retrieving the nodes, and finally achieves the purpose of finding the optimal path. The A* algorithm has high search efficiency for introducing a heuristic function to guide the search direction, omitting the search-independent region. The general expression of the valuation is as follows:

$$f(n) = g(n) + h(n). \tag{1}$$

where $f(n)$ represents the valuation function from the initial point via node n to the target, $g(n)$ represents the actual cost function from the initial point to node n in the state space, and $h(n)$ represents the heuristic estimation cost function of the optimal path from node n to the target.

The search time and accuracy of the A* algorithm are related to the selection of the heuristic function. When the heuristic function $h(n)$ is larger than the actual distance, the number of search nodes decreases, the search efficiency is higher, but the optimal path is not necessarily obtained. When the heuristic function $h(n)$ is less than the actual distance from the node n to the target node, the search nodes increase, the search range is larger, and the optimal solution can be obtained, but the search time is long. Only when the heuristic function $h(n)$ is close to the actual distance from the node n to the target node can the optimal path be quickly and accurately obtained. Considering the flexibility of the cruise ship in the water environment, Euclidean distance is suitable as a heuristic function for the water environment application scenario. The heuristic function calculated from the Euclidean distance is the linear distance from the node n to the target node, which is inevitably no greater than the actual distance from the node n to the target node, so the obtained planning path is the optimal solution.

The cost function $h(n)$ expression represented by the Euclidean distance is as follows:

$$h(n) = \sqrt{(x_n - x_{target})^2 + (y_n - y_{target})^2}. \tag{2}$$

where (x_n, y_n) is the coordinate of the node n in the two-dimensional grid network, and (x_{target}, y_{target}) is the coordinate of the target.

C. THE ARTIFICIAL POTENTIAL FIELD METHOD

The APF method constructs the motion space of the robot into an abstract potential field, in which the target acts as a gravitational source to exert the attractive force on the robot and attracts it to the target; the obstacle acts as a repulsive source to apply a repulsive force to the robot, hindering it from approaching the obstacle. The resultant force of attraction and repulsion acts as a driving force, causing the robot to approach the target while away from obstacles. In this paper, the APF method is mainly used for local path planning of cruise ships. The gravitational field generated by the target covers the entire motion space. The attractive force increases monotonically as the distance between the cruise ship and the target increases. The function expression of the gravitational potential field in two-dimensional motion space is as follows:

$$U_{att}(n) = \frac{1}{2} k_{att} (x_n - x_{target})^2. \tag{3}$$

where k_{att} is the gravitational gain coefficient, where x_n is the position of the cruise ship, and x_{target} is the position of the target.

The expression of the gravitational function corresponding to equation (3) is:

$$F_{att}(n) = -grad[U_{att}(n)] = k_{att}(x_{target} - x_n). \tag{4}$$

where $x_{target} - x_n$ is the distance between the target and the cruise ship.

The limitation of obstacle influence distance results in that the repulsion potential field generated by the obstacle acts in the local range, and the repulsion monotonically decreases as the distance between the cruise ship and the obstacle increases. When the cruise ship exceeds the local range, it is not affected by the repulsion. The function expression of the repulsion potential field is as follows:

$$U_{rep}(n) = \begin{cases} \frac{1}{2} k_{rep} (\frac{1}{x_n - x_o} - \frac{1}{d})^2, & |x_n - x_o| \le d \\ 0, & |x_n - x_o| > d, \end{cases} \tag{5}$$

where k_{rep} is the repulsion gain coefficient, x_o is the position of the obstacle, and d is the obstacle influence distance.

The expression of the repulsion function corresponding to equation (5) is as follows:

$$\begin{aligned} F_{rep}(n) &= -grad[U_{rep}(n)] \\ &= \begin{cases} k_{rep} (\frac{1}{x_n - x_o} - \frac{1}{d}) \frac{1}{(x_n - x_o)^2} \cdot \frac{\partial (x_n - x_o)}{\partial x_n}, \\ \qquad\qquad |x_n - x_o| \le d, \\ 0, \qquad\qquad |x_n - x_o| > d \end{cases} \end{aligned} \tag{6}$$

where $x_n - x_o$ is the distance between the cruise ship and the obstacle.

Therefore, the combined field and resultant force of the cruise ship in the space are as follows:

$$U_{res}(n) = U_{att}(n) + U_{rep}(n). \quad (7)$$

$$F_{res}(n) = F_{att}(n) + F_{rep}(n). \quad (8)$$

The traditional APF method is an effective method to achieve a rapid response to a dynamic environment and has a good application prospect for obstacle avoidance in the case of unknown environments. However, defects of the traditional APF method include that it is easy to obtain an unreachable target [30] or fall into the local minimum problem [31].

III. THE HYBRID PATH PLANNING ALGORITHM

A. ALGORITHM OVERVIEW

The hybrid algorithm proposed in this paper uses the A* algorithm to plan the global path and the improved APF method for unknown regions to achieve the goal of fast obstacle avoidance. The proposed hybrid algorithm's flowchart is shown in Figure 2. First, the current map information is used to construct the grid map model, and the A* algorithm is used to obtain the global planning path from the starting location to the target. When the cruise ship travels along the global path, the equipped sensor detects the surrounding environment in real time and relays environmental information. The detection range of the sensor is 90° in the forward direction. If the surrounding environment is always consistent with the map information, the optimal path can be obtained by smoothing the global planning path. If not, it indicates that the cruise ship is about to enter the unknown areas. For the areas, the current path point is to be the local planning starting point, and the global planning path point in the detection range boundary is seemed as the local target. If the local target is an obstacle area or local path cannot be generated, the grid map is updated with environmental information obtained by the sensor, and the global path is re-planned using the A* algorithm. If the local target is a blank area, the improved APF method is adopted to guide the cruise ship to reach the local target according to the attraction of the target to the cruise ship and the repulsive force generated by obstacles within the detection range and generates a local path. The local path planned by the improved APF method will replace the global path of the same starting point and target. After the replacement, the replaced global path is the optimal path, and the optimal path will be smoothed.

B. THE IMPROVED ARTIFICIAL POTENTIAL FIELD METHOD

After many experimental studies, it is found that the problems existing in the APF method are directly related to the repulsion potential field function [32]. Therefore, the improvement of the repulsion potential field function is the research focus. Inherent defects in the APF method are addressed from

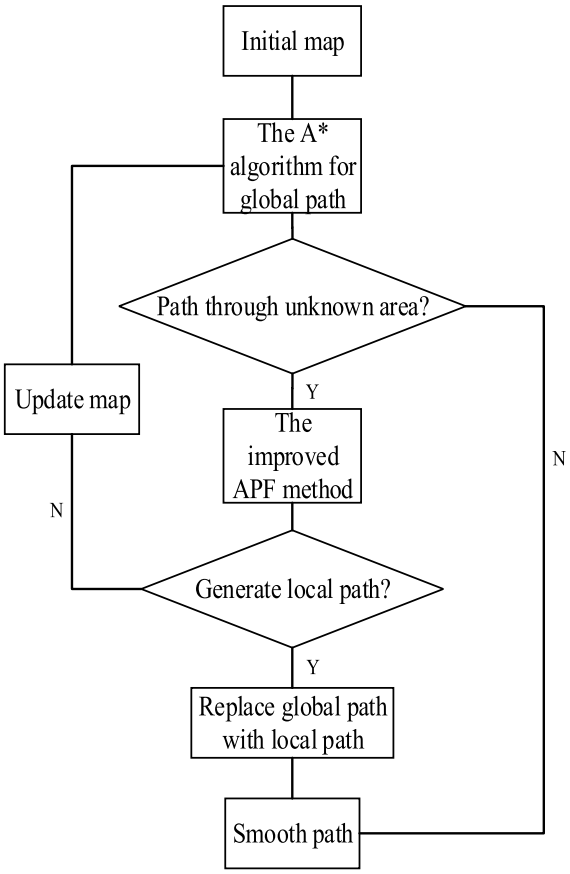

FIGURE 2. The proposed hybrid algorithm flowchart.

two aspects: the construction of the repulsion potential field function and the search strategy of the planning path:

1) REPULSIVE POTENTIAL FIELD FUNCTION OPTIMIZATION

When there is an obstacle near the target and the target is within the repulsive range of the obstacle, the repulsive force near the target is not zero. When the cruise ship approaches the target, its attractive force decreases as the distance from the target decreases, and the repulsive force it receives increases as the distance from obstacle decreases. Since the attractive force of the target is initially greater than the repulsive force of the obstacle, the cruise ship approaches the target, in this progress the attractive force is reduced, and the repulsive force is increased. Then the cruise ship moves away from the obstacles and is attracted to the target by the attractive force. The attractive and repulsive forces alternately play a leading role, causing the cruise ship to reciprocate near the target and lead to the target unreachable problem, as shown in Figure 3. In Figure 3, the obstacles near the target apply a repulsion F_{rep} to the cruise ship, and the target applies an attraction F_{att} to the cruise ship, where $F_{rep} > F_{att}$, so the cruise ship is subjected to the resultant F_{res} away from target.

The repulsion potential field is optimized to satisfy the repulsive force close to zero near the target, and the attractive force always plays a leading role. Therefore, a repulsion

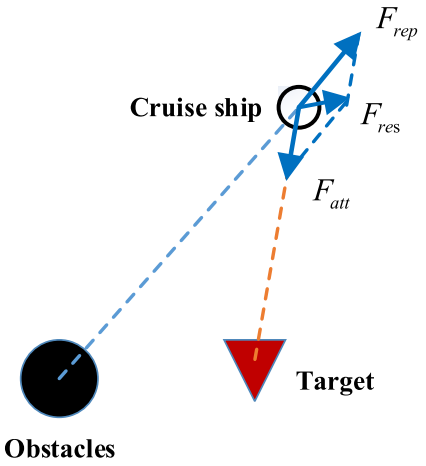

FIGURE 3. Force analysis of the cruise ship in the repulsion potential field function.

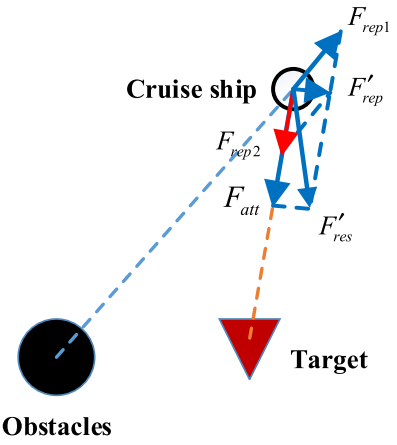

FIGURE 4. Force analysis of the cruise ship in the optimized repulsion potential field function.

correction factor $(x_n - x_{target})^m$ is added to the function of the repulsion potential field, and a new repulsion potential field function obtained by equation (5) is expressed in equation (9).

$$U'_{\text{rep}}(n) = \begin{cases} \frac{1}{2}k_{rep}(\frac{1}{x_n - x_o} - \frac{1}{d})^2(x_n - x_{\text{target}})^m, & |x_n - x_o| \le d \\ 0, & |x_n - x_o| > d, \end{cases} \tag{9}$$

where m is the repulsion correction factor index.

Then, a new repulsion function is obtained from the new repulsion potential field function as follows:

$$F'_{rep}(n) = -grad[U'_{rep}(x_n)] = \begin{cases} F_{rep1} + F_{rep2}, & |x_n - x_o| \le d \\ 0, & |x_n - x_o| > d, \end{cases} \tag{10}$$

In the formula F_{rep1}, F_{rep2} are the repulsion components for the repulsion potential field function. In different directions under the gradient, the specific expression is as follows:

$$F_{rep1}(n) = k_{rep}(\frac{1}{x_n - x_o} - \frac{1}{d})\frac{1}{(x_n - x_o)^2}(x_n - x_{target})^m \cdot \frac{\partial(x_n - x_o)}{\partial x_n}, \tag{11}$$

$$F_{rep2}(n) = \frac{\mathrm{m}}{2}k_{rep}(\frac{1}{x_n - x_o} - \frac{1}{d})^2(x_n - x_{target})^{m-1} \cdot \frac{\partial(x_{target} - x_n)}{\partial x_n}, \tag{12}$$

The new resultant expression for the cruise ship is as follows:

$$F'_{res}(n) = F_{att}(n) + F'_{rep}(n), \tag{13}$$

At this point, the force analysis of the cruise ship is shown in Figure 4.

In the optimized repulsion potential field function, the repulsion provided by the obstacle to the cruise ship can be divided into F_{rep1} away from the obstacle and F_{rep2} pointing to the target. At the environment where obstacles are far away from the target, the ship affected by F_{rep2} and F_{att} can approach the target while away from the obstacles due to F_{rep1}. When the obstacles are close to the target, the repulsive force F_{rep1} of the obstacle is always close to zero. The cruise ship moves toward the target under the action of attraction, which solves the problem of obtaining unreachable targets by the APF method.

2) DIRECTIONAL RANDOM ESCAPE SEARCH STRATEGY

Since the repulsion of the obstacle is limited when the distance between the cruise ship and the obstacle exceeds the obstacles' repulsion range, the cruise ship is not affected by the repulsion, and the global information is not processed in solving the problem of local obstacle avoidance. The counteracting repulsive force and attraction on the cruise ship cause it to stop moving because there is no driving force and be in a local stable state, which is manifested by stopping at a certain point or repeatedly oscillating around it.

Tracking the local path of the cruise ship while it is driving, by setting its moving step size to l when the cruise ship moves n times. Record the current position and the previous step position as x_n, x_{n-1} retrieve the previous M step position x_{n-M} and the position of the front (M-1) step $x_{n-(M-1)}$, where $n > M$. When the cruise ship is caught in local minimum problems, the maximum moving distance does not increase with the number of movements and never exceeds the moving step l, calculate $|x_n - x_{n-M}|$ and $|x_n - x_{n-(M-1)}|$, if $|x_n - x_{n-M}| < l$ and $|x_n - x_{n-(M-1)}| < l$, then the cruise ship is in a local minimum state.

The search strategy in the APF method is improved to address this question. When getting stuck in a local minimum, the escape point is provided as the next moving position, so that the cruise ship is freed from the equilibrium state, and then proceeds to the target according to the new driving force. If it is determined that the cruise ship is in a local

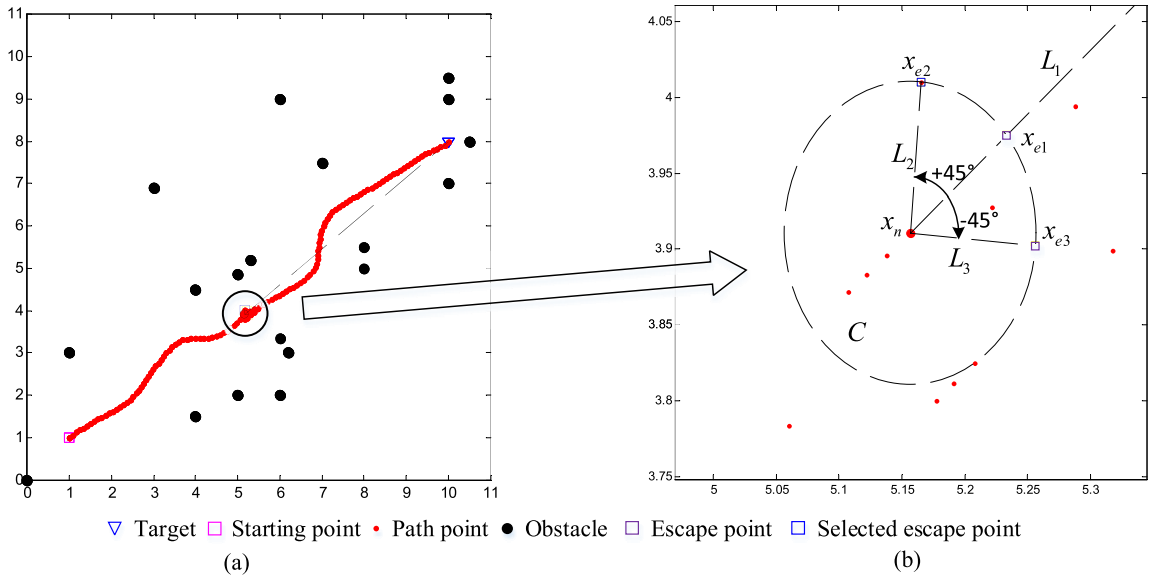

FIGURE 5. (a) The improved APF simulation; (b) Local enlargement.

TABLE 1. Notation to custom symbols.

Notation	
L	Connection
C	Circle
$Line(x,x')$	Connection with x , x' as the endpoint
$Circle(x,r)$	A circle with x as the center and r as the radius
$P_{inter}(L,C,x)$	The intersection of L and C close to point x
$Line(L,x,45°)$	Wire L rotates 45° counterclockwise around x
x_e	Escape point
$\|x\text{-}x'\|$	Euclidean distance between point x and point x'

TABLE 2. The improved APF method path planning implementation.

L1 Establish the gravitational potential field according to formula (3)
L2 Calculate gravity according to formula (4)
L3 Establish an optimized repulsion potential field according to equation (9)
L4 Calculate the repulsive force according to equations (11) and (12)
L5 Calculate the resultant force according to equation (13), and the cruise ship moves in the direction of the resultant force
L6 Repeat L1-L5 steps n times
L7 Fall into a local minimum: **if** $|x_n - x_{n-M}| < l$ and $|x_n - x_{n-(M-1)}| < l$ **then**
L8 $L_1 = Line(x_n, x_{target})$, $C = Circle(x_n, l)$
L_2=$Line(L,x,45°)$, L_3=$Line(L,x,-45°)$
L9 Set the escape points: $x_{e1} = P_{inter}(L_1, C, x_{target})$,
$x_{e2} = P_{inter}(L_2, C, x_{target})$, $x_{e3} = P_{inter}(L_3, C, x_{target})$
L10 Choose a random escape points, **if** the selected escape points is the obstacle area **then**
L11 Choose the other escape points
L12 **else**
L13 Continue to execute downward
L14 **end if**
L15 **else**
L16 **repeat** L1-L7
L17 **until** the local target is reached or the number of iterations is reached
L18 **end if**

stable state, make a line L_1 with the current position x_n, the local minimum point, and the target x_{target}, draw a circle C with x_n as the center of the circle, and the radius is the moving step l. Take the point x_{e1} between the current position x_n and the target x_{target} in the intersection of the straight line L_1 and the circle C. Draw straight lines L_2, L_3 from x_n to circle C, with the line L_1 as the dividing line; the angles formed by the straight lines L_2, L_3 to L_1 are $+45°$ and $-45°$, respectively. At this time, the intersections of the straight lines L_2, L_3 with circle C are x_{e2} and x_{e3}. As shown in Figures 5(a) and 5(b), the cruise ship randomly selects one from the escape points x_{e1}, x_{e2}, and x_{e3} as the next moving position and detaches from the local minimum point while ensuring that the next position is closer to the target. If there is an obstacle at the selected escape point, replace the other escape points which improve the escape success rate of the cruise ship.

Combined with the notation in Table 1, a summary of the improved planning path process for the APF is shown in Table 2:

C. COMBINATION OF THE A* ALGORITHM AND THE IMPROVED APF METHOD

Combining the global path planning ability of the A* algorithm with the local path planning ability of the improved APF method, it is possible to adopt an effective method to obtain an optimal planning path in a short time in the face of a complex environment model. First, use the A* algorithm to plan the global path in the initial grid map. Then retrieve the global path point $\{x_k \,|k = 1, 2, 3 \ldots, N\}$ from the starting

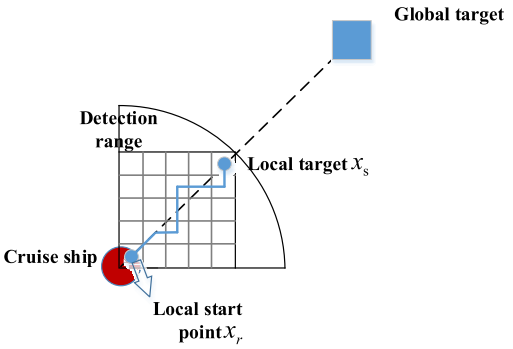

FIGURE 6. Cruise ship sector detection areas.

point x_1. When the next path point x_{r+1} is found at the path point x_r and is located in the unknown area, the starting point is forwardly detected with x_r as the local path, and the detection range is a 90° fan shape in the forward direction and is represented as a 25 grid area in the grid map. The local path planning target is the global path planning point x_s at the detection boundary.

As shown in Figure 6, the improved APF method is used to plan the local path $\{x_k \,|k = r, r+1, \ldots, s\}, 1 \leq r < s \leq N$, for the unknown region within the detection range. The resulting partial path will replace the global path from x_r to x_s.

D. SENSOR-BASED SELF-LEARNING ABILITY

The self-learning function, shown in Table 3, is used at the following situations. One is that the obstacle is overlapped with the local target so that the improved APF method cannot plan a local path. The other one is when a local target is determined, but a local path cannot be generated because of local environmental limitations. In this cases, the sensor updates the detected map information from the original map, and the global path is re-planned by using the A* algorithm based on the updated map, which contains more known environment information, as shown in Figures 7(a) and (b). The Figure 7(a) presents the situation that the local target planned by the hybrid algorithm proposed in this paper is obstacle areas after detecting in the unknown regions. In this case, the improved APF method cannot be adopted due to the lack of the local target. Therefore, on the basis of updating the map information, the A* algorithm is admitted to re-plan the global path to complete the path planning in the unknown area. As shown in Figure 7(b), the path planned by the improved APF method is close to the local target under the resultant force of obstacles and local target in the local environment. However, for the environment limitation formed by obstacles, no path could be generated to approach local target in unknown regions, and a complete local path cannot be obtained by the improved APF method. Then, the initial map is updated according to the map information within the detection of the sensor, and the A* algorithm is used to complete the path re-planning of the obstacle regions.

Therefore, the self-learning ability based on sensor proposed in this paper greatly increases path planning

TABLE 3. Self-learning ability realization process.

```
L1 if local target = obstacle area then
L2     Updating map
L3     A* algorithm for re-planning
L4 else
L5     Improved APF method for local path planning
L6     if local path not generated then
L7         Updating map
L8         A* algorithm for re-planning
L9     else
L10        Replacing the part of global path with local path
L11    end if
L12 end if
```

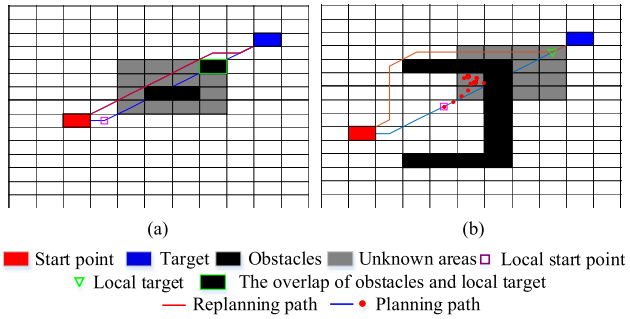

FIGURE 7. Cruise ship sector detection areas. (a) Re-planning for the overlapping situation that local target planned by the hybrid algorithm proposed in this paper is obstacle areas after detection in the unknown regions; (b) Re-planning for the situation that the local planning path is not generated.

capability for complex environments. The combination of the A* algorithm and the improved APF overcomes the deficiencies of the traditional APF method when dealing with different obstacles distribution on scenarios.

E. OPTIMAL PATH SMOOTHING

There are numerous redundant points in the optimal path of the hybrid algorithm proposed in this paper. The length of optimal path can be shortened by smoothing the optimal path and eliminating redundant points. Combined with the notation in Table 1, the smoothing process is shown in Table 4 and the specific steps are as follows: (1) retrieve the path points $\{x_k \,|k = 1, 2, 3 \ldots, N\}$ from the starting point x_1 along the planned path to the target x_N; (2) check adjacent obstacles of points x_1 and x_2, to make sure that if the connection between x_1 and x_2 is at a safe distance from the surrounding obstacles, then continue to search next point until the line connecting x_1 and x_m, $(m < N)$ passes through the obstacle; (3) take x_1 and x_{m-1} as the endpoints, and replace the original path between x_1 and x_{m-1} with the line which links the same endpoints and choosing x_{m-1} as a new starting point to continue to check the path point forward; (4) repeat the above steps until the target is reached.

F. ALGORITHM PROCEDURES OF THE PROPOSED METHOD

The detailed algorithm procedures of the proposed hybrid algorithm is shown in Table 5.

TABLE 4. Optimal path smoothing process implementation process.

L1 Retrieving path points $\{x_k \mid k = 1, 2, 3..., N\}$
L2 Setting endpoint x_k
L3 **repeat** checking the path point forward
L4 **until** $Line(x_k, x_m)$, $m < N$ pass through the obstacles
L4 Setting anchor point $x_{m\text{-}1}$
L5 Replacing the part of global path with $Line(x_k, x_{m\text{-}1})$
L6 Setting new endpoint $x_{m\text{-}1}$
L7 **repeat** L3-L6
L8 **until** reaching the target

TABLE 5. Algorithm procedures of the proposed method.

1. Create a raster map model
   1) The map size is 30×30
   2) The passable area is represented with white grids, the obstacle area is represented with black grids, and the unknown area is represented with gray grids
2. Plan global path
   1) Set the heuristic function
   2) A* algorithm
3. Retrieve whether the global path passes through an unknown area
   Yes, planning a local path
   No, retrieve the next path point
4. Employ improved APF method to plan local path
   1) Set the local start point and the local target point, and retrieve whether the local target point is in an obstacle area
      Yes, sensor-based self-learning is shown in Table 3 L1-L3
      No, the improved APF method is shown in Table 2 L1-L18
   2) Determine whether to generate a partial path
      Yes, replace the global path having the same local start and target
      No, sensor-based self-learning is shown in Table 3 L6-L8
5. Smooth the global path as shown in Table 4 L1-L8

IV. SIMULATION EXPERIMENTS

Comparative experiments are carried out on the simulation map of the *Yantouzhu Scenic Spot* in *Taihu Lake* and *Qixing Lake*, part of *Dongting Lake*

The simulation experiment takes Windows 10 as the software platform and MATLAB R2016b as the simulation tool. The hardware platform is Intel Core E5-2620 V3 processor, with 2.4G main frequency and 32GB memory. The simulation parameters are presented in Table 6.

A. SIMULATION IN ORDINARY ENVIRONMENT

The traditional A* algorithm, the traditional APF method, the improved APF method, the pseudo-bacterial potential field (PBPF) [33] and the proposed algorithm of this paper are used to plan the path on the grid map (30 × 30) with unknown regions. The experimental results are shown in Figures 8−12 and Table 7.

In order to prove the validity of the experimental results, we run each algorithm 30 times in the same environments. The best, mean, worst and standard deviation results of path planning time and distance are shown in Table 8. Moreover, the t-test is performed to check whether the algorithms are statistically different or not [34]. Level 0.05 of significance is considered, and significance difference is represented by '+' in the Table.

TABLE 6. Simulation parameters.

Symbol	Definition	Numerical value
n_s	Starting position	(3,1) (1,4)
n_g	Target's position	(20,30) (79,78)
$c(n_k, n_{k-1})$	Adjacent nodes cost function	Euclidean distance
$g(n_k)$	Actual cost function	$c(n_k, n_{k-1})+g(n_{k-1})$
$h(n_k)$	Heuristic estimation cost function	Euclidean distance
$D(n_k)$	Direction of detection	direction in X axis: $\frac{(\vec{x}_{\text{target}} - \vec{x}_k)}{\lvert x_{\text{target}} - x_k \rvert}$ direction in Y axis: $\frac{(\vec{y}_{\text{target}} - \vec{y}_k)}{\lvert \vec{y}_{\text{target}} - \vec{y}_k \rvert}$
z	Detection zone	5 × 5 grids
k_{att}	Attraction gain coefficient	15
k_{rep}	Repulsion gain coefficient	4.2
m	Repulsion's correction factor index	2
d	Obstacle influence distance	2.5
l	Simulation step size	0.5

TABLE 7. Simulation experiment algorithm performance comparison.

Algorithm name	Path planning time t/s	Path planning distance d/m
The traditional A algorithm*	1.3050	360.9160
The traditional APF method	0.4269	----
The improved APF method	0.3233	540.0000
The PBPF algorithm	1.8326	361.3550
The hybrid algorithm	0.4952	360.4957

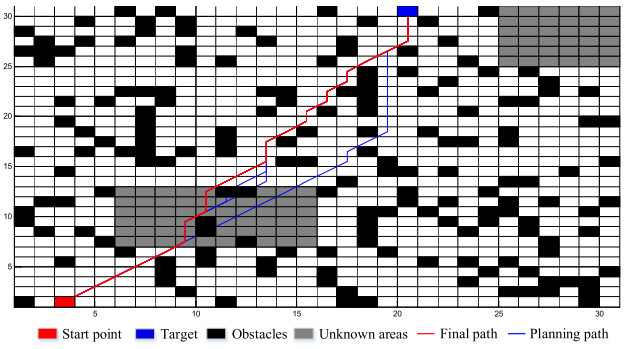

FIGURE 8. Simulation result based on the traditional A* algorithm.

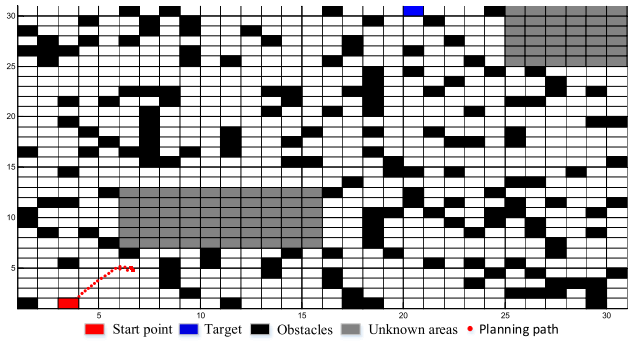

FIGURE 9. Simulation result based on the traditional APF method.

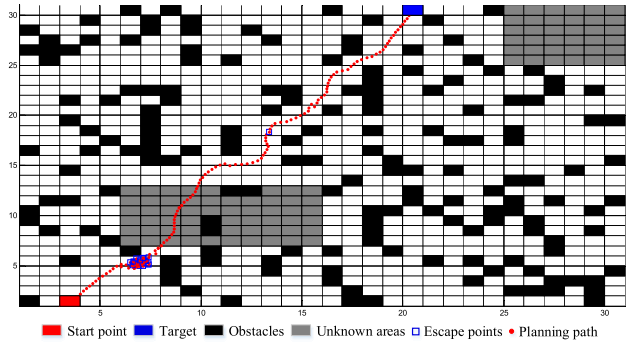

FIGURE 10. Simulation result based on the improved APF method.

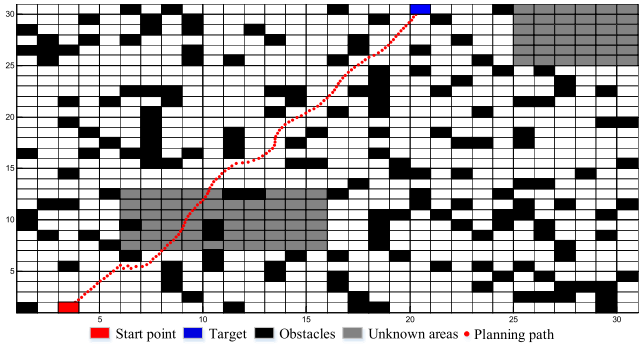

FIGURE 11. Simulation result based on the PBPF algorithm.

B. RESULT ANALYSIS IN ORDINARY ENVIRONMENT

Figures 8-12 show the path planning results of different algorithms from the same starting point to the same target under the same experimental conditions. The performance comparison of the simulation experiment results shown in Table 7 is a record of the path planning time and path planning distance data for the corresponding algorithms in Figures 8-12. At the same time, Table 8 describes the statistical characteristics of the four algorithms.

In the simulation environment where a large number of obstacles exist (illustrated in Figure 9), the traditional APF method has a planning time of only 0.4269 s. This has great advantages in planning time cost compared with other methods, but the resultant force generated by the obstacles and the target during the planning process is zero. The cruise ship repeatedly oscillates in a region after leaving the starting point and cannot reach the target. The traditional A* algorithm in Figure 8 plans a global path based on the initial map, then detects the unknown area once the path point is within unknown region and updates the map information based on the path point. Since the global path passes through the obstacle areas, it is not an effective travel path, and it is necessary to perform secondary planning in the updated map. Due to the limited detection range, the A* algorithm repeatedly detects and updates the map to the unknown area and obtains the optimal path without obstacles in the 4th path plan after 4 times detection, and the optimal path (360.9160 m) is obtained. The A* algorithm consumes a lot of time (1.3050 s) for repeated uses, so it has poor time performance indicators. In Figure 10, the improved APF method uses a large number of escape points to avoid the cruise ship plunging into a local minimum state. Because the directional random escape strategy has a simple structure, the use of a large number of escape points does not impose a large burden on path planning time. The time performance can be optimal (0.3233 s) and the target can be reached even if there are obstacles around the target. However, a large number of escape points in the figure are concentrated in the same area, which is not conducive to navigation in the actual background, and the obtained collision-free path is not the optimal result in path planning distance performance (540.000 m). The PBPF is the state-of–the-art potential based algorithm. With the evolution rules, the optimal path is found in path planning distance (361.3550 m) in Figure 11, while the time cost (1.8362 s) which is worse than the improved APF method apparently could be improved. Figure 12 shows that the proposed algorithm first uses the A* algorithm to obtain the global path. When the global path passes through the unknown region, the local starting point and the local target are selected to obtain the local path by the improved APF method, which is used twice, since the unknown area is larger than the detection range. And the partial global path is replaced by the local path in the same starting point and target. A local path planning avoids obstacles and reduces the repeated planning of the A* algorithm, which is then smoothed to achieve an optimal path and reduce the path planning distance. The smoothing

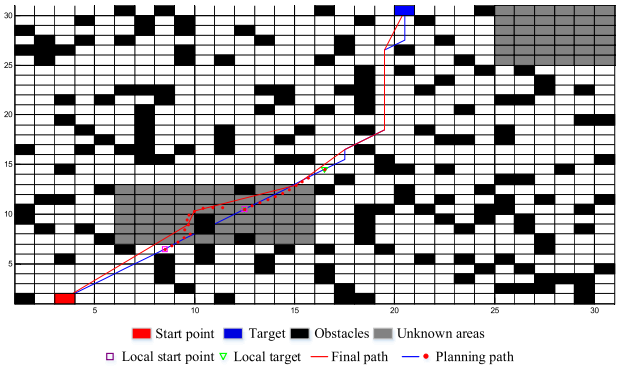

FIGURE 12. Simulation result based on the proposed algorithm.

TABLE 8. Statistical analysis of algorithms.

Performance indicators	*Statistics*	*The traditional A* algorithm*	*The improved APF method*	*The PBPF algorithm*	*The hybrid algorithm*
Path planning time t/s	Best	1.3050	0.3233	1.8326	0.4952
	Mean	1.3882	0.4836	1.9185	0.5082
	Worst	1.4693	0.5930	2.0371	0.5752
	Std. Dev.	0.0328	0.0828	0.0567	0.0192
	t-test	3.33e-43(+)	0.114	2.96e-42(+)	---
Path planning distance d/m	Best	360.9160	423.0000	349.3550	360.4957
	Mean	360.9160	514.8000	371.7431	360.9243
	Worst	360.9160	615.0000	402.8790	360.9390
	Std. Dev.	0	44.594	17.1334	0.0035
	t-test	-----	7.89e-18(+)	2e-3(+)	---

TABLE 9. Simulation experiment comparison in complex environment.

Algorithm name	Path planning time t/s	Path planning distance d / m
The ACO algorithm	2055.63	1153.3815
The hybrid algorithm	21.5233	1184.3271

work makes the optimal path decrease the steering angle as well.

Combined with Table 8, the proposed hybrid algorithm inherits the advantage of the improved APF method in time cost, so there is not significant difference shown in statistical data compared with the improved APF method. Meanwhile, the A* algorithm's statistical results in distance cost is not obtained due to its non-normal distribution, but the mean results of the proposed hybrid algorithm (360.9243 m) is close to the A* algorithm's (360.9160 m),which proves the proposed algorithm has the advantage of A* algorithm in path planning distance. As for other aspects, comparing with the three algorithms, it can be observed that the hybrid algorithm proposed in this paper outperforms in the test environment from the mean solutions and the p-values which are far smaller than the level 0.05 of significance.

C. SIMULATION IN COMPLEX ENVIRONMENT

In order to show the performance of the combined algorithm in the complex environment, the path planning on the grid map (80×80) with unknown regions is simulated, which presents the simulation map of *Qixing Lake*, part of *Dongting Lake*. For comparison, the parameters of the classical ACO algorithm [35] are set as follows: the information elicitation factor $\alpha = 1$, the expected heuristic factor $\beta = 7$, the evaporation factor $\rho = 0.3$, the pheromone intensity $Q = 1$. To ensure the ACO algorithm can get better planning results, the number of ants $m = 200$, the iterations $k = 100$, and the detection range of each ant is set as 5×5 grid map size. The simulation results are shown in Figures 13, 14 and Table 9.

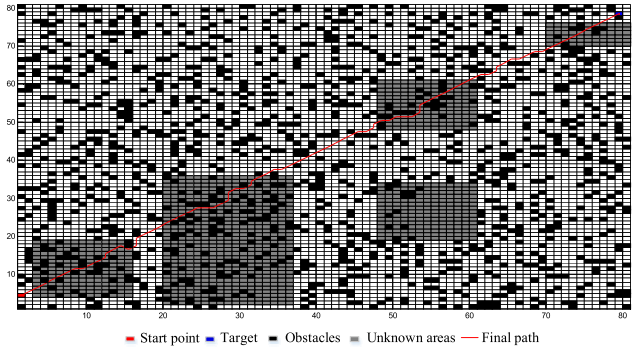

FIGURE 13. Simulation result of path planning based on the ACO algorithm in complex environment.

D. RESULT ANALYSIS IN COMPLEX ENVIRONMENT

Figures 13 and 14(a) present the path planning results of the ACO algorithm and the proposed hybrid algorithm, where the complex environment contains 5 unknown regions and different types of path planning problems caused by uneven distribution of obstacles. Figures 14(b)-14(e), which are the partial enlarged areas of Figure 14(a) marked by blue rectangle borders, explain the detailed planning process of the hybrid algorithm proposed in this paper when to solve path planning problems under different distributions of obstacles. The order from Figure 14(b) to Figure 14(e) corresponds to the blue border areas from the start point to the target. Table 9 records the path planning time and path planning distance data of the ACO algorithm and the proposed hybrid algorithm.

It can be seen from the simulation results that both the ACO algorithm and the proposed hybrid algorithm avoid obstacles successfully and complete the path planning from the start point to the target in a complex environment. To approach the lowest planning path instead of local optimal solutions in path planning distance, the ACO algorithm spends more time (2055.63 s) to explore unknown areas and update whole map information. Its own algorithm structure leads to slow convergence speed, and wide range environment dramatically increase the computing time as well. In the exploration of ants near the starting point, due to the long distance between ants and the target, the state

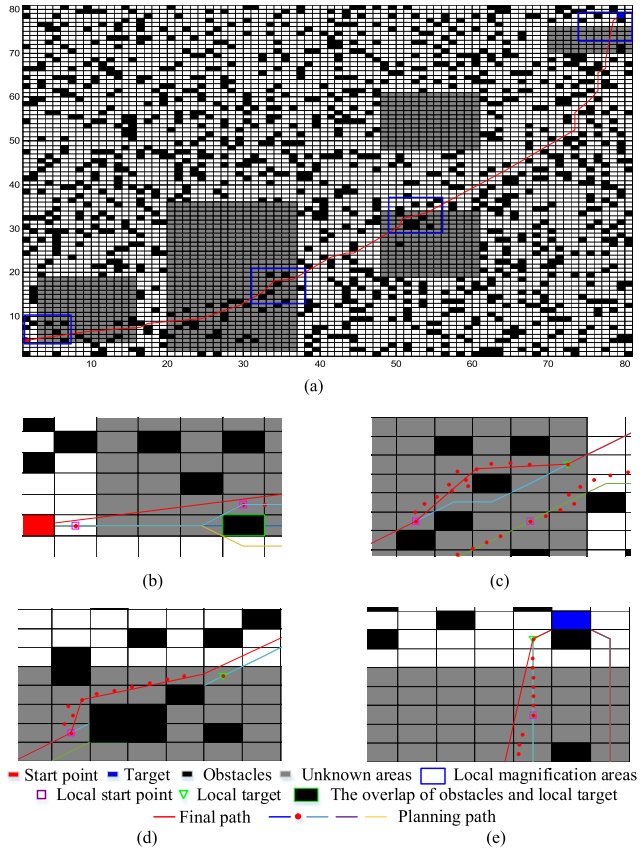

FIGURE 14. (a) Simulation results of path planning based on the hybrid algorithm in complex environment; (b)-(e) Local magnification areas' planning progress of Figure 14(a) in the order from the start point to the target.

transition rule of the ACO algorithm increases the randomness of ants' movement to the surrounding areas instead of moving toward the target, so the unknown areas close to the start point in Figure 13 are almost completely detected. With continuously updating map information, the ACO algorithm gradually converges to the optimal path (1153.3815 m). Figure 14(a) displays the final optimal path generated by the hybrid algorithm, which renews finite map information to obtain optimal path result (1184.3271 m) in path planning distance. Furthermore, the smoothed path is conducive to the actual movement of the cruise ship. Compared with the ACO algorithm, the proposed hybrid algorithm has greater advantage in planning time (21.5233 s). Such a method solves various types of planning problems in unknown regions, which appears great applicability in the environment of dense obstacles distribution. The four blue marked areas in Figure 14(a) from the start point to the target correspond to Figures 14(b)-(e) respectively, which describe the specific planning processes to deal with path planning problems in unknown environments. In the case exhibited in Figure 14(b) that the local target overlaps with the obstacle after detecting an unknown areas, the sensor-based self-learning ability is used to update map information and re-plan global path. In Figure 14(c), the improved APF method in the proposed hybrid algorithm achieves the path planning from the local start point to the target in the channel shaped area formed by obstacles without oscillating points. Figure 14(d) shows that the proposed hybrid algorithm has great application in local path planning of unknown areas where large number of obstacles exist. Figure 14(e) shows that when the obstacles are near the target, the path points planned by the proposed hybrid algorithm can go straight to the local target affected by attractive force and the target unreachable problem is solved. Combined with the above analysis, it can be concluded that the hybrid algorithm proposed in the paper can accomplish path planning in complex environment with unknown areas, and the path planning distance result is close to the results obtained by the ACO algorithm. Meanwhile, the proposed algorithm has optimal performance in planning time cost.

E. PARAMETERS DISCUSSION

In the proposed hybrid algorithm, the parameters in the improved APF method affect the path planning results in the aspects of path planning distance and path planning time. For simulation map shown in this paper, the map scale is 1 grid representing 10 meters. Setting detection zone to 5×5 grids which is 50×50 meters in reality is consistent with the practical situation. The obstacle influence distance which is 25 meters could provide enough reaction time to achieve obstacle avoidance for cruise ships. The step size which is 5 meters in reality is suitable for cruise ships to avoid crash accidents to obstacles.

To exam influences parameters k_{att}, k_{rep} and m on path planning distance and time, a completely unknown environment is established based on Figure 1. By referring to [36] the optimal range of k_{att} and k_{rep} under unknown circumstance is estimated. The detailed variations of parameters on path planning distance and path planning time are shown in Figures 15-17.

The results from Figure 15 indicate that as the increase of gravitational gain coefficient k_{att}, the change of path planning distance and time is irregular due to complex environment formed by distribution of obstacles. And obstacles avoidance could not be accomplished at the time gravitational gain coefficient k_{att} is set big. It is observed that repulsion gain coefficient k_{rep} keeps the balance on path planning performance and obstacles avoidance in Figure 16. It is easy to earn shorter path planning distance and time while k_{rep} is within 4, but cruise ship can be below the safe distance of obstacles in this environment which leads to the failure of obstacles avoidance. As shown in Figure 17, the repulsion's correction index m presents the same features with k_{rep}. When m is between 1.4 and 2, the improved APF algorithm keeps safe distance from obstacles. Meanwhile, optimal path planning distance and time are obtained.

F. CONCLUSIONS

In this paper, a hybrid path planning algorithm combined with the A* algorithm and an improved APF method is proposed

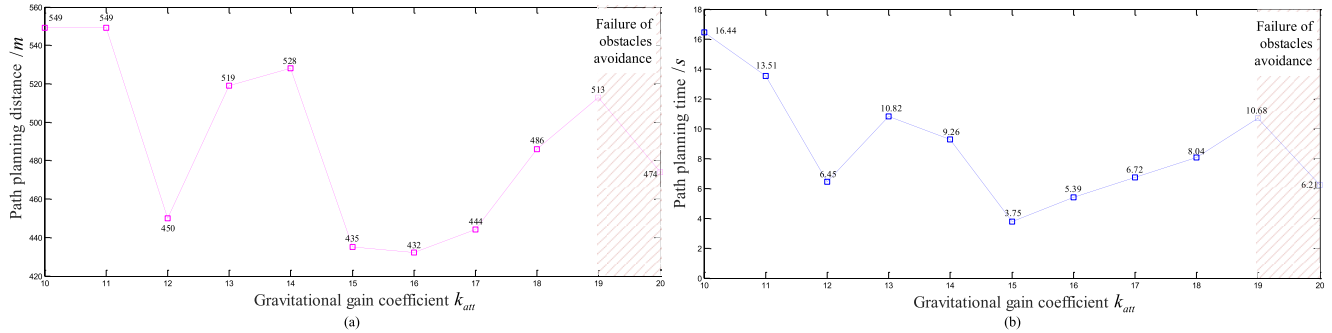

FIGURE 15. The impact of k_{att} on path planning distance and time when k_{rep} and m are constant. (a) The variations of path planning distance; (b) The variations of path planning time.

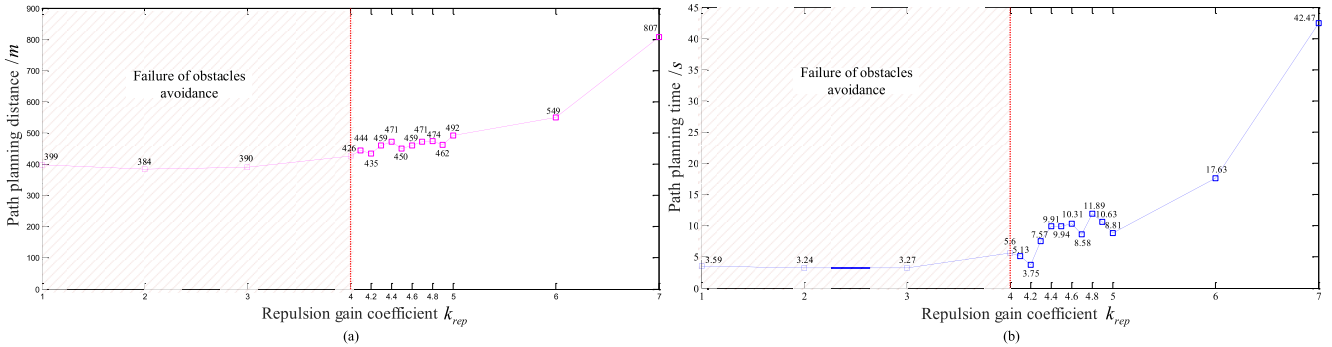

FIGURE 16. The impact of k_{rep} on path planning distance and time when k_{att} and m are constant. (a) The variations of path planning distance; (b) The variations of path planning time.

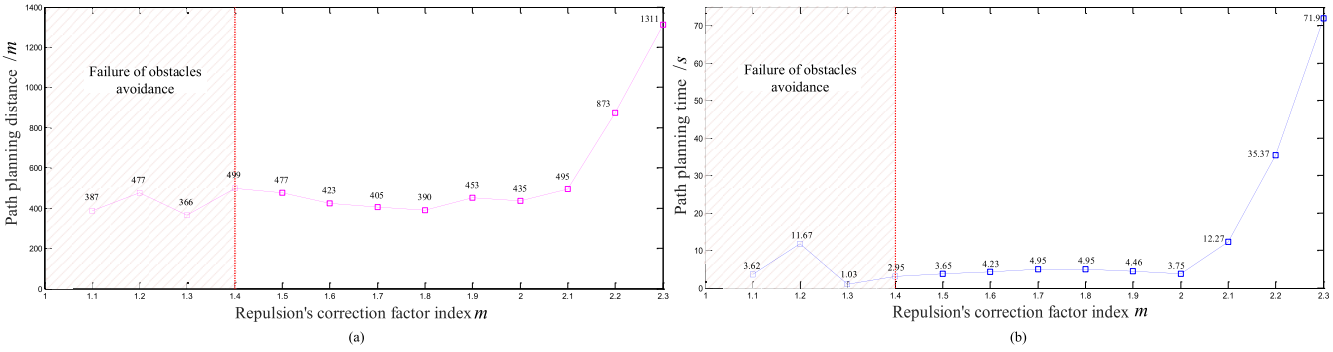

FIGURE 17. The impact of m on path planning distance and time when k_{att} and k_{rep} are constant. (a) The variations of path planning distance; (b) The variations of path planning time.

to solve the problem of an unmanned cruise ship's water quality sampling in complex environment. The experiments are designed to challenge the hybrid algorithm in this paper in ordinary and complex scenarios. To achieve a fair comparison between the proposed algorithm and the other methods, exhaustive statistical experiments are conducted. In the situation of ordinary environments, the simulation results also show that the proposed algorithm is superior to the other methods in the comprehensive performance of path planning distance and path planning time. In the case of complex environments, the simulation results demonstrate the good ability of the proposed hybrid algorithm in path planning with different obstacles distribution, the comparison with the A* algorithm, the traditional APF method, the improved APF method, the PBPF algorithm and the ACO algorithm shows that it provides the best solutions in less time when obtaining optimal path distance.

As for future work, path planning in dynamic environments is willing to be studied, since this work only considers unknown static environments. Another future work is to use irregular graphics to model obstacles, which can extend the proposed algorithm to more complex environment.

REFERENCES

[1] N. Sariff and N. Buniyamin, "An overview of autonomous mobile robot path planning algorithms," in *Proc. IEEE Res. Develop.*, Jun. 2006, pp. 183–188.

[2] Z. Zhu, J. Xiao, J.-Q. Li, F. Wang, and Q. Zhang, "Global path planning of wheeled robots using multi-objective memetic algorithms," *Integr. Comput.-Aided Eng.*, vol. 22, no. 4, pp. 387–404, 2015.

[3] J.-D. Zhang, Y.-J. Feng, F.-F. Shi, G. Wang, B. Ma, R.-S. Li, and X.-Y. Jia, "Vehicle routing in urban areas based on the oil consumption weight-Dijkstra algorithm," *IET Intell. Transp. Syst.*, vol. 10, no. 7, pp. 495–502, 2016.

[4] Y. Chen and J.-Y. Chen, "Application of Jacobian defined direct interaction coefficient in DRGEP-based chemical mechanism reduction methods using different graph search algorithms," *Combustion Flame*, vol. 174, pp. 77–84, Dec. 2016.

[5] A. Tharwat, M. Elhoseny, A. E. Hassanien, T. Gabel, and A. Kumar, "Intelligent Bézier curve-based path planning model using chaotic particle swarm optimization algorithm," *Cluster Comput.*, no. 4, pp. 1–22, 2018.

[6] M. Elhoseny, A. Tharwat, and A. E. Hassanien, "Bezier curve based path planning in a dynamic field using modified genetic algorithm," *J. Comput. Sci.*, vol. 25, pp. 339–350, Mar. 2018.

[7] F. Zheng, A. C. Zecchin, J. P. Newman, H. R. Maier, and G. C. Dandy, "An adaptive convergence-trajectory controlled ant colony optimization algorithm with application to water distribution system design problems," *IEEE Trans. Evol. Comput.*, vol. 21, no. 5, pp. 773–791, Oct. 2017.

[8] Y. Zhao, Z. Zheng, and Y. Liu, "Survey on computational-intelligence-based UAV path planning," *Knowl.-Based Syst.*, vol. 158, pp. 54–64, Oct. 2018.

[9] Y. Wang, P. Yao, and Y. Dou, "Monitoring trajectory optimization for unmanned surface vessel in sailboat race," *Optik*, vol. 176, pp. 394–400, Jan. 2019.

[10] P. Yao and S. Zhao, "Three-dimensional path planning for AUV based on interfered fluid dynamical system under ocean current (June 2018)," *IEEE Access*, vol. 6, pp. 42904–42916, 2018.

[11] P. Yao, H. Wang, and Z. Su, "UAV feasible path planning based on disturbed fluid and trajectory propagation," *Chin. J. Aeronaut.*, vol. 28, no. 4, pp. 1163–1177, 2015.

[12] M. Wang and J. N. K. Liu, "Fuzzy logic-based real-time robot navigation in unknown environment with dead ends," *Robot. Auto. Syst.*, vol. 56, no. 7, pp. 625–643, 2008.

[13] J. Ni, L. Wu, P. Shi, and S. X. Yang, "A dynamic bioinspired neural network based real-time path planning method for autonomous underwater vehicles," *Comput. Intell. Neurosci.*, vol. 2017, Feb. 2017, Art. no. 9269742.

[14] X. Yu, W.-N. Chen, T. Gu, H. Yuan, H. Zhang, and J. Zhang, "ACO-A*: Ant colony optimization plus A* for 3D traveling in environments with dense obstacles," *IEEE Trans. Evol. Comput.*, to be published.

[15] T. T. Mac, C. Copot, D. T. Tran, and R. D. Keyser, "A hierarchical global path planning approach for mobile robots based on multi-objective particle swarm optimization," *Appl. Soft Comput.*, vol. 59, pp. 68–76, Oct. 2017.

[16] W. Khaksar, S. Vivekananthen, K. S. M. Saharia, M. Yousefi, and F. B. Ismail, "A review on mobile robots motion path planning in unknown environments," in *Proc. IEEE Int. Symp.*, Oct. 2015, pp. 295–300.

[17] O. Motlagh, D. Nakhaeinia, S. H. Tang, B. Karasfi, and W. Khaksar, "Automatic navigation of mobile robots in unknown environments," *Neural Comput. Appl.*, vol. 24, nos. 7–8, pp. 1569–1581, 2014.

[18] O. A. Abubakr, M. A. K. Jaradat, and M. A. Hafez, "A reduced cascaded fuzzy logic controller for dynamic window weights optimization," in *Proc. IEEE 11th Int. Symp. Mechatronics Appl. (ISMA)*, Mar. 2018, pp. 1–4.

[19] P. K. Mohanty and D. R. Parhi, "A new hybrid intelligent path planner for mobile robot navigation based on adaptive neuro-fuzzy inference system," *Austral. J. Mech. Eng.*, vol. 13, no. 3, pp. 195–207, 2015.

[20] J. Li, G. Deng, C. Luo, Q. Lin, Q. Yan, and Z. Ming, "A hybrid path planning method in unmanned air/ground vehicle (UAV/UGV) cooperative systems," *IEEE Trans. Veh. Technol.*, vol. 65, no. 12, pp. 9585–9596, Dec. 2016.

[21] L. Yang, J. Qi, D. Song, J. Xiao, J. Han, and Y. Xia, "Survey of robot 3D path planning algorithms," *J. Control Sci. Eng.*, vol. 2016, Mar. 2016, Art. no. 5.

[22] M. Elbanhawi, M. Simic, and R. Jazar, "Randomized bidirectional B-spline parameterization motion planning," *IEEE Trans. Intell. Transp. Syst.*, vol. 17, no. 2, pp. 406–419, Feb. 2016.

[23] K. Wei and B. Ren, "A method on dynamic path planning for robotic manipulator autonomous obstacle avoidance based on an improved RRT algorithm," *Sensors*, vol. 18, no. 2, p. 571, 2018.

[24] H. Wang, Z. Wang, L. Yu, Q. Wang, and C. Liu, "A hybrid algorithm for robot path planning," in *Proc. IEEE Int. Conf. Mechatronics Automat.*, Aug. 2018, pp. 986–990.

[25] C.-C. Kao, C.-M. Lin, and J.-G. Juang, "Application of potential field method and optimal path planning to mobile robot control," in *Proc. IEEE Int. Conf. Autom. Sci. Eng.*, Aug. 2015, pp. 1552–1554.

[26] J. K. Park and J. Kim, "Collision avoidance method for UAV using A* search algorithm," in *Advances in Intelligent and Interactive Systems and Applications*. Cham, Switzerland: Springer, 2018, pp. 186–193.

[27] P. Kaiser, J. Wegner, A. Lucchi, M. Jaggi, T. Hofmann, and K. Schindler, "Learning aerial image segmentation from online maps," *IEEE Trans. Geosci. Remote Sens.*, vol. 55, no. 11, pp. 6054–6068, Nov. 2017.

[28] D.-Q. Zhu and M.-Z. Yan, "An overview of path planning technology for mobile robots," *Control Decis.*, vol. 25, no. 7, pp. 961–967, 2010.

[29] I. Chabini and S. Lan, "Adaptations of the A* algorithm for the computation of fastest paths in deterministic discrete-time dynamic networks," *IEEE Trans. Intell. Transp. Syst.*, vol. 3, no. 1, pp. 60–74, Mar. 2002.

[30] D. Li, Z. Zhou, H. Deng, C. Wang, K. Li, C. Wang, and P. Teng, "2D obstacle avoidance method for snake robot based on modified artificial potential field," in *Proc. IEEE Unmanned Syst. Int. Conf.*, Oct. 2017, pp. 358–363.

[31] R. Zappulla, H. Park, V.-L. Josep, and M. Romano, "Real-time autonomous spacecraft proximity maneuvers and docking using an adaptive artificial potential field approach," *IEEE Trans. Control Syst. Technol.*, to be published.

[32] T. T. Mac, C. Copot, D. T. Tran, and R. De Keyser, "Heuristic approaches in robot path planning: A survey," *Robot. Auto. Syst.*, vol. 86, pp. 13–28, Dec. 2016.

[33] U. Orozco-Rosas, O. Montiel, and R. Sepúlveda, "Pseudo-bacterial potential field based path planner for autonomous mobile robot navigation," *Int. J. Adv. Robot. Syst.*, vol. 12, no. 7, p. 81, 2015.

[34] U. Orozco-Rosas, O. Montiel, and R. Sepúlveda, "Mobile robot path planning using membrane evolutionary artificial potential field," *Appl. Soft Comput.*, vol. 77, pp. 236–251, Apr. 2019.

[35] R. Uriol and A. Moran, "Mobile robot path planning in complex environments using ant colony optimization algorithm," in *Proc. IEEE 3rd Int. Conf. Control, Autom. Robot.*, Apr. 2017, pp. 15–21.

[36] O. Montiel, U. Orozco-Rosas, and R. Sepúlveda, "Path planning for mobile robots using bacterial potential field for avoiding static and dynamic obstacles," *Expert Syst. Appl.*, vol. 42, no. 12, pp. 5177–5191, 2015.

JIABIN YU received the B.S. degree from the Beijing Technology and Business University, Beijing, China, in 2007, the M.S. degree in automation from the Beijing Institute of Technology, in 2009, and the Ph.D. degree in control theory and control engineering from the Institute of Automation, Chinese Academy of Sciences, in 2012. He has been an Associate Professor with the Beijing Technology and Business University, since 2017. His current research interests cover water environment evaluation and prediction, motor control, and complex system design.

WEI DENG received the B.S. degree in electrical engineering and automation from the Beijing Technology and Business University, Beijing, China, in 2017, where he is currently pursuing the master's degree. His current research interest includes path planning of mobile equipment.

ZHIYAO ZHAO received the B.S. degree in automation from the Beijing Technology and Business University, Beijing, China, in 2011, and the Ph.D. degree in guidance, navigation, and control from the School of Automation Science and Electrical Engineering, Beihang University, Beijing, in 2017. He has been a Lecturer with the Beijing Technology and Business University, since 2017. His current research interests include water environment evaluation and prediction, system health management, and stochastic hybrid systems.

XIAOYI WANG received the B.S. degree in automation from the Department of Automation, Shenyang College of Technology, Shenyang, China, in 2000, the M.S. degree in optics from Shanxi University, Shanxi, China, in 2003, and the Ph.D. degree in control theory and control engineering from the School of Automation, Beijing Institute of Technology, Beijing, China, in 2006. He has been a Professor with the Beijing Technology and Business University, since 2013. His current research interests include water environment modeling, optimization and decision-making, and optimal control.

JIPING XU received the B.S. and M.S. degrees in automation from the Beijing Technology and Business University, Beijing, China, in 2002 and 2005, respectively, and the Ph.D. degree in control theory and control engineering from the School of Automation, Beijing Institute of Technology, Beijing, in 2010. He has been an Associate Professor with the Beijing Technology and Business University, since 2010. His current research interests include water environment evaluation and prediction, and big data analysis.

LI WANG received the Ph.D. degree from the School of Reliability and System Engineering, Beihang University, Beijing, China, in 2011. She is currently with the Beijing Technology and Business University. Her current research interest includes complex systems modeling analysis and prediction.

QIAN SUN received the B.E. degree in measurement and control technology and instrument from the Harbin Institute of Technology, in 2007, and the Ph.D. degree in instrument science and technology from Beihang University, in 2014. Since 2014, she has been with the College of Computer and Information Engineering, Beijing Technology and Business University, as a Lecturer. Her research interests include water quality sensor networks, and water environment evaluation.

ZHE SHEN received the B.S. degree in electrical engineering and automation from the Institute of Disaster Prevention Science and Technology. He is currently pursuing the master's degree with the Beijing Technology and Business University. His current research interest includes water environment evaluation and prediction.